ENERGY RESOURCES

10.1126/sciadv.1400129

N-doped carbon nanomaterials are durable catalysts for oxygen reduction reaction in acidic fuel cells

Jianglan Shui, Min Wang, Feng Du, Liming Dai*

The availability of low-cost, efficient, and durable catalysts for oxygen reduction reaction (ORR) is a prerequisite for commercialization of the fuel cell technology. Along with intensive research efforts of more than half a century in developing nonprecious metal catalysts (NPMCs) to replace the expensive and scarce platinum-based catalysts, a new class of carbon-based, low-cost, metal-free ORR catalysts was demonstrated to show superior ORR performance to commercial platinum catalysts, particularly in alkaline electrolytes. However, their large-scale practical application in more popular acidic polymer electrolyte membrane (PEM) fuel cells remained elusive because they are often found to be less effective in acidic electrolytes, and no attempt has been made for a single PEM cell test. We demonstrated that rationally designed, metal-free, nitrogen-doped carbon nanotubes and their graphene composites exhibited significantly better long-term operational stabilities and comparable gravimetric power densities with respect to the best NPMC in acidic PEM cells. This work represents a major breakthrough in removing the bottlenecks to translate low-cost, metal-free, carbon-based ORR catalysts to commercial reality, and opens avenues for clean energy generation from affordable and durable fuel cells.

INTRODUCTION

The molecular oxygen reduction reaction (ORR) is important to many fields, such as energy conversion (for example, fuel cells, metal-air batteries, and solar cells), corrosion, and biology (*1*, *2*). For fuel cells to generate electricity by electrochemically reducing oxygen and oxidizing fuel into water, cathodic oxygen reduction plays an essential role in producing electricity and is a key limiting factor on the fuel cell performance (*3*–*5*). To construct fuel cells of practical significance, efficient catalysts are required to promote the ORR at cathode (*6*–*8*). Traditionally, platinum has been regarded as the best catalyst for fuel cells, although it still suffers from multiple drawbacks, including its susceptibility to time-dependent drift and MeOH crossover and CO poisoning effects (*4*, *9*). However, the large-scale practical application of fuel cells cannot be realized if the expensive platinum-based electrocatalysts for ORR cannot be replaced by other efficient, low-cost, and durable electrodes.

Cobalt phthalocyanine was reported as the ORR electrocatalyst in alkaline electrolytes in 1964 (*5*, *10*). Since then, the search for nonprecious metal catalysts (NPMCs) with transition metal/nitrogen/carbon (M-N*x*/C, typically $x = 2$ or 4, M = Co, Fe, Ni, Mn) complex catalytic sites as low-cost alternatives to Pt for electrochemical reduction of oxygen in fuel cells has attracted long-term interest. Although tremendous progress has been made and a few recently reported NPMCs show electrocatalytic performance comparable to that of Pt (*11*–*14*), most of the NPMCs are still too expensive and/or far away from satisfaction in durability for practical applications. Those NPMCs of high catalytic activities often exhibit fast decay under somewhat challenging testing/operation conditions, such as at a constant voltage of 0.5 V with pure oxygen as cathode fuel (*11*, *13*), and relatively good durability has only been observed under less efficient working conditions with a relatively low potential (for example, 0.4 V) and/or diluted oxygen (air) as the cathode fuel (*14*).

Center of Advanced Science and Engineering for Carbon (Case4Carbon), Department of Macromolecular Science Engineering, Case School of Engineering, Case Western Reserve University, 10900 Euclid Avenue, Cleveland, OH 44106, USA.
*Corresponding author: E-mail: liming.dai@case.edu

Along with intensive research efforts of more than half a century in developing nonprecious metal ORR catalysts, a new class of metal-free ORR catalysts based on carbon nanomaterials has been discovered (*1*) and attracted worldwide attention (*15*–*33*), which, as alternative ORR catalysts, could markedly reduce the cost and increase the efficiency of fuel cells. In particular, it was found that vertically aligned nitrogen-doped carbon nanotube (VA-NCNT) arrays can act as a metal-free electrode to catalyze a $4e^-$ ORR process with a three times higher electrocatalytic activity and better long-term stability than commercially available platinum/C electrodes (for example, C2-20, 20% platinum on Vulcan XC-72R; E-TEK) in an alkaline electrochemical cell (*1*). These carbon-based metal-free ORR catalysts are also free from the CO poisoning and methanol crossover effects.

Quantum mechanics calculations with B3LYP hybrid density functional theory and subsequent experimental observations indicated that the carbon atoms adjacent to nitrogen dopants in the NCNT structure had a substantially high positive charge density to counterbalance the strong electronic affinity of the nitrogen atom (*1*). A redox cycling process reduced the carbon atoms that naturally exist in an oxidized form, followed by reoxidation of the reduced carbon atoms to their preferred oxidized state upon O_2 absorption and reduction, leading to a reduced ORR potential. Furthermore, the N doping–induced charge transfer from adjacent carbon atoms could change the chemisorption mode of O_2 from an usual end-on adsorption (Pauling model) at the pure CNT surface to a side-on adsorption (Yeager model) of O_2 onto the NCNT electrode to effectively weaken the O-O bonding for efficient ORR (*1*). Hence, doping carbon nanomaterials with heteroatoms as in the NCNT electrodes could efficiently create the metal-free active sites for electrochemical reduction of O_2.

Recent worldwide research activities (*15*–*33*) in this exciting field have not only confirmed the above findings but also further proved that the doping-induced charge transfer has large impact on the design/development of new metal-free electrocatalytic materials, including various heteroatom-doped CNTs (*1*, *19*), graphene (*16*, *20*, *21*), and graphite (*22*–*28*) for fuel cell and many other applications (*29*–*31*). High

electrocatalytic activity comparable or even superior to commercial Pt/C electrodes and excellent tolerance to MeOH crossover and CO poisoning effects have been demonstrated for many of the carbon-based metal-free ORR catalysts in electrochemical half-cells with alkaline electrolytes. Nevertheless, the large-scale applications of the carbon-based metal-free ORR catalysts in practical fuel cells cannot be realized if they do not have an adequate long-term durability and high ORR performance in acidic polymer electrolyte membrane (PEM) fuel cells, which currently serve as the mainstream fuel cell technology of great potential for large-scale applications in both transport and stationary systems (*9*). As yet, however, the performance evaluation (for example, electrocatalytic activity and long-term operational stability) of carbon-based metal-free ORR catalysts in actual PEM fuel cells has been largely ignored. This is presumably because carbon-based metal-free ORR catalysts are often found to be less effective in acidic electrolytes with respect to alkaline media, and it is quite challenging to make them sufficiently effective for single-cell testing in acidic PEM fuel cells.

In spite of this, we demonstrated here that both the VA-NCNT array and a rationally designed nitrogen-doped graphene/CNT composite (N-G-CNT) as the cathode catalysts in acidic PEM fuel cells exhibited remarkably high gravimetric current density comparable to the most active NPMCs. Because carbon is much more anti-corrosive to acids than most transition metals, the VA-NCNT array and N-G-CNT composite further showed a significantly durable performance, even with pure H_2/O_2 gases, in acidic PEM fuel cells, outperforming their NPMC counterparts. Therefore, carbon-based metal-free catalysts hold great potential as low-cost, efficient, and durable ORR catalysts to replace Pt in practical PEM fuel cells.

RESULTS

VA-NCNT arrays have been previously reported to show excellent ORR performance (*1*), even superior to the commercially available Pt/C electrodes, in electrochemical half-cells with alkaline electrolytes, as also confirmed by the VA-NCNTs used in this study (figs. S1 to S3). To carry out the performance evaluation of VA-NCNTs in PEM fuel cells, we made the VA-NCNT arrays (80 μm in height, a surface packing density of 0.16 mg cm^{-2}) into a membrane electrode assembly (MEA) at the highest allowable catalyst loading of 0.16 mg cm^{-2}. Figure 1 schematically shows procedures for the MEA preparation (Fig. 1A), along with a typical scanning electron microscopic (SEM) image of the starting VA-NCNT array (Fig. 1B) and a photographic image of the newly developed MEA (Fig. 1C), whereas the MEA fabrication details are given in the Supplementary Materials. Briefly, we first performed the electrochemical oxidation in H_2SO_4 to remove Fe residue, if any, in the VA-NCNTs made from pyrolysis of iron(II) phthalocyanine (*1*), followed by etching off the purified VA-NCNT array from the Si wafer substrate in aqueous hydrogen fluoride [10 weight percent (wt %)], rinsing it copiously with deionized water, transferring it onto a gas diffusion layer [GDL; Carbon Micro-porous Layer (CMPL), ElectroChem Inc.], and drop-coating with a sulfonated tetrafluoroethylene-based ionomer "Nafion" (DuPont) as binder and electrolyte, which was then assembled with a Pt/C-coated GDL as the anode and an intermediate layer of proton-conductive membrane (Nafion N211, DuPont) as the separator (see the Supplementary Materials for detailed preparation and fig. S4 for the MEA cross-section images). As can be seen in Fig. 1 (A to C) and fig. S4, the NCNT ORR catalyst within the MEA thus produced largely retained its vertical alignment.

The resulting MEA containing the VA-NCNT metal-free ORR electrocatalysts was evaluated in an acidic PEM fuel cell operating with the Nafion electrolyte and pure H_2/O_2 gases. To start with, the PEM fuel cell was activated after 100 scanning cycles from open circuit potential (OCV) to ~0.1 V (Fig. 1D). To our surprise, a consistent polarization performance was observed for more than 5100 scanning cycles, indicating a stable electrocatalytic performance even in acid under the harsh working condition. Thus, N-C centers in the carbon-based metal-free catalysts seem to be more stable than the transition metal active sites in NPMCs in PEM fuel cells (*34*, *35*). The relatively poor polarization performance seen in Fig. 1D for the first 10 cycles is, most probably, due to the weak electrode-electrolyte interaction on the as-prepared hydrophobic

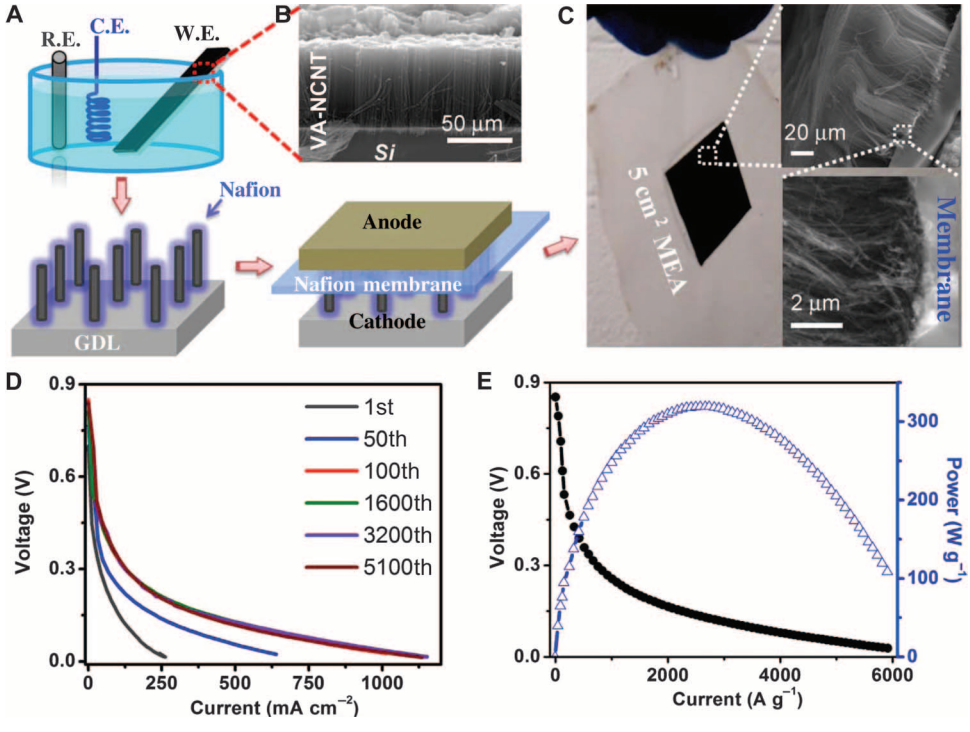

Fig. 1. Fabrication of MEA of VA-NCNT arrays and its performance in a PEM fuel cell. (**A**) Schematic drawings for the fabrication of MEA from VA-NCNT arrays (0.16 mg cm^{-2}) and the electrochemical oxidation to remove residue Fe. C.E., counter electrode; R.E., reference electrode; W.E., working electrode. (**B**) Typical SEM image of the VA-NCNT array. (**C**) Digital photo image of the used MEA after durability test with the cross-section SEM images shown in the inserts. (**D**) Polarization curves as the function of the areal current density after accelerated degradation by repeatedly scanning the cell from OCV to 0.1 V at the rate of 10 mA s^{-1}. (**E**) Polarization and power density as the function of the gravimetric current density. Cathode catalyst loading 0.16 mg cm^{-2}, Nafion/VA-NCNT = 1/1. H_2/O_2: 80°C, 100% relative humidity, 2-bar back pressure.

VA-NCNT electrode, which became hydrophilic upon electrochemical activation during the subsequent polarization cycles (*36*). For the VA-NCNT MEA, significantly high gravimetric current densities were observed: 35 A g^{-1} at 0.8 V, 145 A g^{-1} at 0.6 V, and 1550 A g^{-1} at 0.2 V (Fig. 1E). As can also be seen in Fig. 1E, the peak power density was 320 W g^{-1} for our VA-NCNT MEA, outperforming or comparable to even the most active NPMC catalysts (Table 1) (*11*).

As a building block for CNTs, the two-dimensional (2D) single atomic carbon sheet of graphene with a large surface area and peculiar electronic properties is an attractive candidate for potential uses in many areas where CNTs have been exploited. Thus, heteroatom-doped graphene has quickly emerged as another class of interesting carbonaceous metal-free ORR catalysts (*16*) soon after the discovery of electrocatalytic activity of VA-NCNTs (*1*). Superior to CNTs, the one-atom-thick graphene sheets have all constituent carbon atoms at the surface to enhance the surface area and a 2D planar geometry to further facilitate electron transport (*37*), and hence very effective electrocatalysis. Although graphene sheets with a large surface area and excellent charge transport properties are ideal electrocatalytic materials for ORR after doping with appropriate heteroatoms (for example, B, S, N, and/or P) (*16*, *20*, *38*), much of the graphene surface area and the associated catalyst sites are lost because of restacking via the strong π-π interaction if the graphene sheets are not physically separated to preserve the high surface area intrinsically associated with individual graphene sheets. Along with others (*37*, *39*), we have prepared 3D graphene-CNT self-assemblies (doped with or without heteroatoms) of large surface/interface areas and well-defined porous network structures as electrode materials with fast ion diffusion and efficient electron transport for energy conversion and storage (*31*, *40*–*42*), including metal-free ORR catalysts (*43*).

Because excellent ORR performance, particularly in alkaline media, has also been demonstrated for graphene-based metal-free ORR catalysts (*17*, *43*), it is highly desirable to also evaluate their performance in actual PEM fuel cells in acidic media. For this purpose, we first prepared metal-free graphene oxide (GO) suspension by the modified Hummers' method (*31*), which was then mixed with oxidized CNT suspension, prepared from commercially available nonaligned multiwalled CNTs (Baytubes C 150 HP, Bayer MaterialScience) after purification to remove metal residues, to produce metal-free porous N-doped graphene and CNT composites (N-G-CNT) through freeze-drying, followed by annealing at 800°C in NH_3 for 3 hours (see the Supplementary Materials for details and fig. S5). The N-G-CNT–based catalyst ink for MEAs was then prepared by mixing 2.5 mg of N-G-CNT catalyst with 10 mg of carbon black particles [primary particle radius, 34 nm; BET (Brunauer-Emmett-Teller) surface area, 1270 m^2 g^{-1}; Ketjenblack EC-600JD] and 375 mg of Nafion solution (5%) in 1.5 ml of deionized water and isopropanol mixture (volume ratio = 1:2). Thereafter, the ink was sonicated for 10 min and stirred overnight, then painted onto a 5-cm^2 GDL as the cathode electrode, and assembled into a MEA with a Pt/C-coated GDL as the anode and an intermediate layer of proton-conductive membrane (Nafion N211, DuPont) as the separator for subsequent testing (fig. S6). Several synergistic effects can arise from the above fabrication process to maximize the utilization of catalyst sites in the N-G-CNT composite: (i) N-G can prevent N-CNTs from the formation of the bundle structure to facilitate the dispersion of N-CNTs by anchoring individual N-CNTs on the graphene sheets via the strong π-π stacking interaction (fig. S5, A to D); (ii) N-CNTs can also effectively prevent the N-G sheets from restacking by dispersing CNTs on the graphene basal plane to make more rigid curved N-G-CNT sheets than the N-G sheets (fig. S5, C to F); and (iii) the addition of carbon black (Ketjenblack) can not only further separate N-G-CNT sheets in the catalyst layer but also induce continued porous multichannel pathways between the N-G-CNT sheets for efficient O_2 diffusion (Fig. 2). A comparison of fig. S6F with fig. S6C indicates that the introduction of carbon black particles led to a porous network structure for the N-G-CNT/KB catalyst layer, facilitating the O_2 diffusion (see also, Fig. 2, A to D). BET measurements on the electrodes showed that a 5-cm^2 porous cathode N-G-CNT/KB@GDL has a surface area of 155 m^2 g^{-1} (or 1161 m^2 g^{-1} after taking off the weight of GDL and Nafion) and a significant number of pores from micro- to macrosizes (Fig. 2, E and F). In contrast, a dense cathode N-G-CNT@GDL without interspersed carbon black particles has a surface area as low as 16 cm^2 g^{-1} with negligible pore volume. The presence of pores in Fig. 2 (C and D) could facilitate the mass transfer of O_2 gas in the porous N-G-CNT/KB catalyst layer (Fig. 2G) with respect to the densely packed N-G-CNT sheets (Fig. 2, A and B) without the intercalated carbon black (Fig. 2H).

Before the single-cell performance evaluation, we carried out the rotating disc electrode (RDE) and rotating ring-disc electrode (RRDE) tests for the newly developed N-G-CNT metal-free catalyst in a three-electrode electrochemical cell. Figure 3A reproduces typical cyclic voltammetric (CV) curves of the N-G-CNT, showing a large cathodic peak at 0.8 V in O_2-saturated 0.1 M KOH solution, but not N_2-saturated electrolyte. The onset potential of the N-G-CNT is as high as 1.08 V, nearly 80 mV higher than that of Pt/C (Fig. 3B). Half-wave potential of the N-G-CNT is 0.87 V, 30 mV higher than that of Pt/C. Therefore, the N-G-CNT shows excellent electrocatalytic performance in 0.1 M KOH, even better than the commercial Pt/C electrode (C2-20, 20% platinum on Vulcan XC-72R; E-TEK), via a one-step $4e^-$ ORR process

Table 1. The gravimetric activities of various transition metal–derived NPMCs compared with the metal-free VA-NCNT and N-G-CNT + KB in PEM fuel cells. All the data in the table have also been scaled by the electrode surface area.

Materials	Current at 0.8 V (A g^{-1})	Current at 0.2 V (A g^{-1})	Peak power density (W g^{-1})	Catalyst loading (mg cm^{-2})	O_2-H_2 back pressure (bars)	Reference
FeCo/N/C	15	700	200	2	1.0	(*14*)
Fe/N/C	8/100	800/2500	233/400	3.9/0.9	0.5	(*11*)
Fe/N/C	15	325	80	4	1.3	(*45*)
VA-NCNT	35	1550	320	0.16	1.5	This work
N-G-CNT + KB	30	1500	300	0.5	1.5	This work

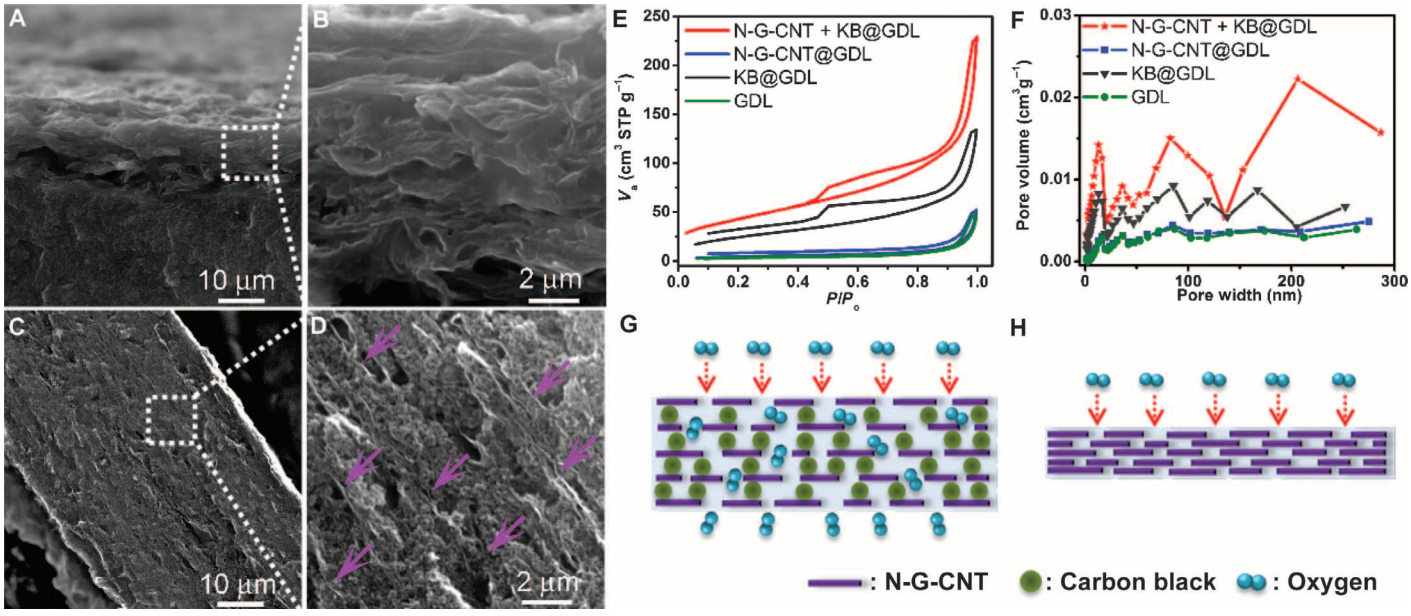

Fig. 2. Morphological features of the N-G-CNT electrodes with and without the addition of Ketjenblack. (**A** to **D**) Cross-section SEM images of (A and B) the densely packed catalyst layer of N-G-CNT/Nafion (0.5/0.5 mg cm^{-2}) and (C and D) the porous catalyst layer of N-G-CNT/KB/Nafion (0.5/2/2.5 mg cm^{-2}). Purple arrows in (D) indicate the parallelly separated N-G-CNT sheets with interdispersed porous KB agglomerates. (**E** and **F**) BET surface areas (E) and pore volume distributions (F) of a piece of 5-cm^2 GDL, GDL with KB (2 mg cm^{-2}), GDL with N-G-CNT (0.5 mg cm^{-2}), and GDL with N-G-CNT/KB (0.5/2 mg cm^{-2}) as indicated in the figures. (**G** and **H**) Schematic drawings of the MEA catalyst layer cross section, showing that O_2 efficiently diffused through the carbon black separated N-G-CNT sheets (G) but not the densely packed N-G-CNT sheets (H).

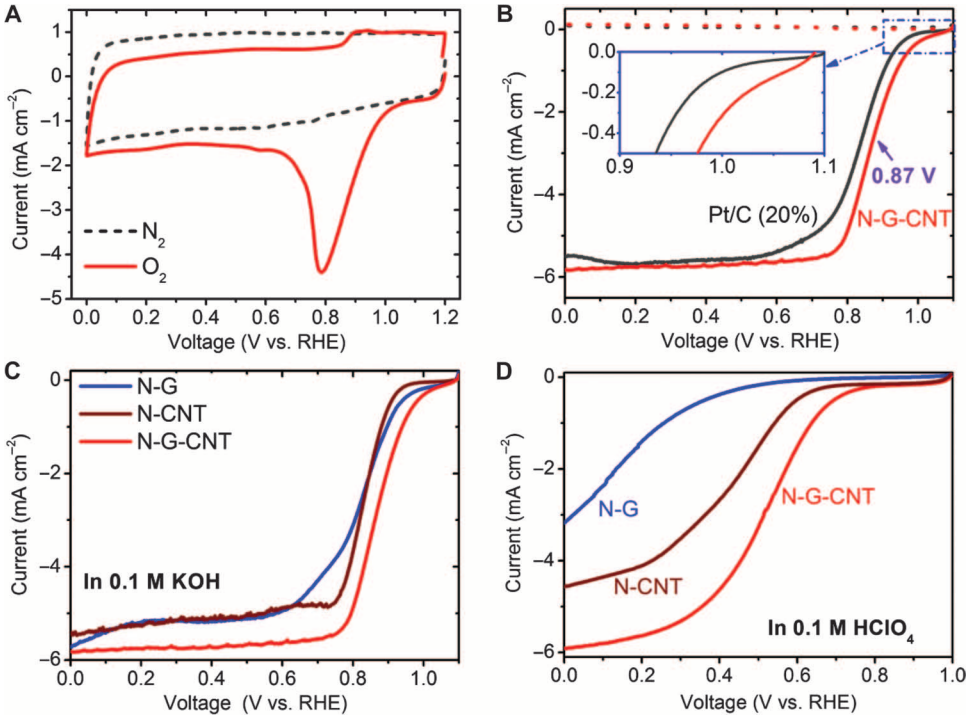

Fig. 3. Electrocatalytic activities of the carbon-based metal-free catalysts in half-cell tests. (**A**) CVs of the N-G-CNT in O_2- or N_2-saturated 0.1 M KOH. (**B**) Linear sweep voltammetry (LSV) curves of the N-G-CNT compared with Pt/C (20%) electrocatalyst by RRDE in O_2-saturated 0.1 M KOH solution at a scan rate of 10 mV s^{-1} and a rotation speed of 1600 rpm. (**C** and **D**) LSV curves of the N-G and N-CNT compared with the N-G-CNT in O_2-saturated 0.1 M KOH (C) and 0.1 M $HClO_4$ (D).

(fig. S7) with a better stability as well as a higher tolerance to MeOH crossover and CO poisoning effects than the Pt catalyst (fig. S8). As far as we are aware, these results are the highest records for metal-free graphene and CNT ORR catalysts. As expected, the N-G-CNT composite also exhibited much better ORR performance than that of N-CNT and N-G catalysts in both the alkaline (Fig. 3C) and acidic media (Fig. 3D) because of its unique foam-like 3D architecture formed in the thin composite layer on the RDE electrode even without the addition of carbon black in the absence of mechanical compression (fig. S9, vide infra) because 3D carbon networks have been previously demonstrated to facilitate electrocatalytic activities (*31*, *43*). More detailed ORR performance of the N-G-CNT in acidic media with respect to Fe/N/C and Pt/C can be found in fig. S10.

The above results indicate that N-G-CNT holds great potential for oxygen reduction in practical fuel cells. Therefore, we further carried out the performance evaluation on MEAs based on the N-G-CNT in a 5-cm^2 PEM fuel cell with pure H_2/O_2 as fuel gases at 80°C. At a typical catalyst loading of 2 mg cm^{-2} (*11*–*14*, *44*), the cell limiting current was as low as 700 mA cm^{-2},

although the cell OCV reached 0.97 V (fig. S11A). We found that the addition of carbon black (KB, 2 mg cm^{-2}) into the N-G-CNT catalyst layer in the MEA caused ~85% improvement on the delivered current density at a low voltage range (<0.4 V), although KB itself had negligible electrocatalytic activity (fig. S11A). The above observed enhancement in the current output can be attributed to the KB-induced porous network formation to enhance the O_2 diffusion (Fig. 2, D and G, and fig. S6F) because the porosity seen in fig. S9F for the as-cast N-G-CNT single electrode has been significantly reduced within the corresponding MEA (fig. S6C) prepared under mechanical pressing (see the Supplementary Materials for the MEA preparation). The improved electrocatalytic performance was also supported by the reduced cell impedance for the N-G-CNT + KB with respect to its N-G-CNT counterpart (fig. S11B).

The cell performances at the N-G-CNT loading of 0.5 and 2 mg cm^{-2} plus KB (2 mg cm^{-2}) are comparable (Fig. 4A), indicating a marked activity suppression at the high catalyst loading even with carbon black dispersing. When the catalyst loading was further reduced to 0.15 mg cm^{-2}, however, the catalytic sites in the cathode were not sufficient to support a normal polarization curve. Figure 4B shows the gravimetric polarization and power density curves for the N-G-CNT in the presence of carbon black (N-G-CNT/KB/Nafion = 0.5:2:2.5 mg cm^{-2}), from which a current of 30 A g^{-1} at 0.8 V, a limiting current of 2000 A g^{-1} at 0.1 V, and a peak power density of 300 W g^{-1} were obtained. Although metal-free catalysts usually exhibited a lower catalytic activity than did NPMCs in RDE measurements (*45*), the observed gravimetric activity of the N-G-CNT + KB is comparable to high-performance Fe(Co)/N/C catalysts (Table 1 and fig. S12, A to C), attributable to the full utilization of catalytic sites in the rationally designed N-G-CNT + KB catalyst layer with the enhanced multichannel O_2 pathways (Fig. 2, D and G, and fig. S6F). The 3D multichannel porous structure, together with the unique materials hybridization, makes the PEM fuel cell based on the N-G-CNT + KB cathode to show a much better cell performance than do its counterparts with the cathode made from either of the constituent components (that is, N-G + KB and N-CNT + KB, respectively) (fig. S13).

Finally, the N-G-CNT + KB was further subjected to the durability test in the acidic PEM fuel cells at a constant voltage of 0.5 V with pure H_2/O_2 as fuel gases (Fig. 4C) in comparison with the Fe/N/C NPMC (see the Supplementary Materials for preparation). Like VA-NCNT, the N-G-CNT + KB exhibited an excellent stability with a relatively small current decay (~20% decay over 100 hours; Fig. 4C). In contrast, the Fe/N/C catalyst showed an initial sharp current decay with a total of about 75% decay over 100 hours at both the high (2 mg cm^{-2}) and low loadings (0.5 mg cm^{-2}). Excellent durabilities were observed for the N-G-CNT + KB catalyst at both low and high loadings (Fig. 4C and fig. S14).

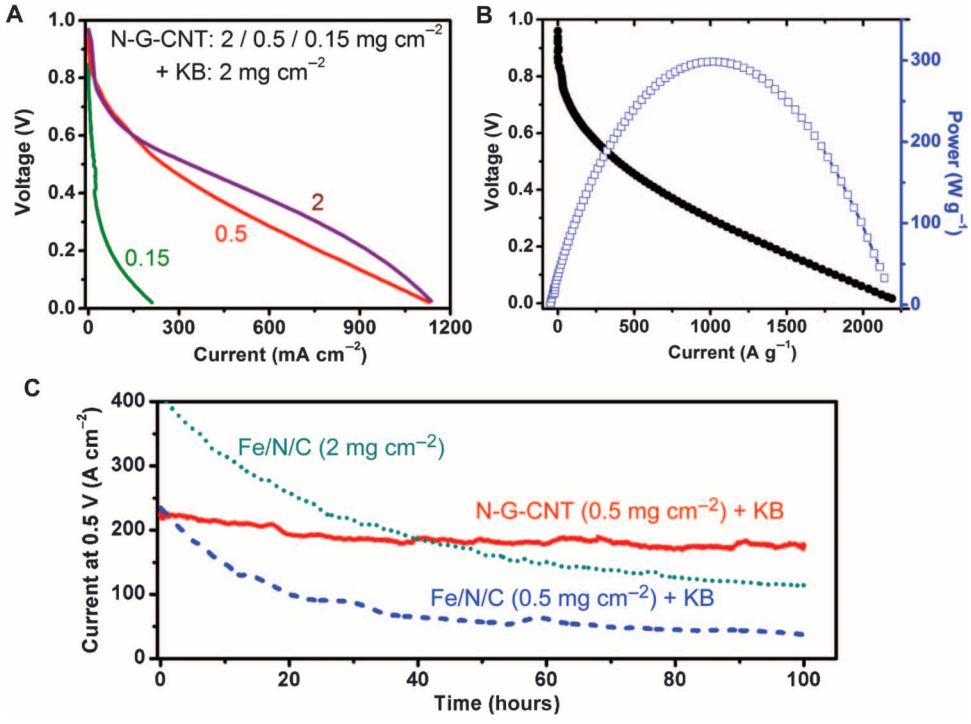

Fig. 4. Power and durability performance of N-G-CNT with the addition of KB in PEM fuel cells. (**A**) Polarization curves of N-G-CNT with loadings: 2, 0.5, or 0.15 mg cm^{-2} plus KB (2 mg cm^{-2}) for each cathode. The weight ratio of (N-G-CNT/KB)/Nafion = 1/1. (**B**) Cell polarization and power density as the function of gravimetric current for the N-G-CNT/KB (0.5/2 mg cm^{-2}) with the weight ratio of (N-G-CNT/KB)/Nafion = 1/1. (**C**) Durability of the metal-free N-G-CNT in a PEM fuel cell measured at 0.5 V compared with a Fe/N/C catalyst (see the Supplementary Materials for preparation details). Catalyst loading of N-G-CNT/KB (0.5 mg cm^{-2}) and Fe/N/C (0.5 and 2 mg cm^{-2}). Test condition: H_2/O_2: 80°C, 100% relative humidity, 2-bar back pressure.

DISCUSSION

The fast performance drop at the first 20 hours for the Fe/N/C catalyst was typical for NPMCs (*5*, *11*, *45*, *46*) because of detrimental effects of the acidic and strong reduction environments on the metal active centers at the PEM fuel cell cathode (*34*). Because the N-G-CNT + KB catalytic sites are free from metal nanoparticle (fig. S15), no significant acidic corrosion is envisioned for the carbon electrode because carbon is much more anti-corrosive to acids than most transition metals. Therefore, the observed excellent stabilities for both N-G-CNT + KB and VA-NCNT cathodes in PEM fuel cells should be an important intrinsic character for the carbon-based metal-free catalysts, facilitating them for a large variety of practical applications. These results show great potential for carbon-based metal-free catalysts to be used as low-cost, efficient, and durable ORR catalysts in practical PEM fuel cells. Furthermore, the VA-NCNT and N-G-CNT + KB catalysts used in this study shared similar features in that N-doped carbon nanomaterials were used for the high ORR electrocatalytic activities, and that the porous structures with a large surface area were rationally designed for enhanced electrolyte/reactant diffusion. The methodology developed here can be regarded as a general approach for the development of

a large variety of high-performance, low-cost, metal-free catalysts for various practical energy devices, particularly in PEM fuel cells.

MATERIALS AND METHODS

VA-NCNT was synthesized by pyrolysis of iron(II) phthalocyanine according to our previously published procedures (*1*). N-G-CNT composite was synthesized by sequentially combining a modified Hummers' method for the GO fabrication (*31*), freeze-drying a mixture of GO and oxidized CNT, followed by annealing at 800°C in NH_3 for 3 hours. The preparation details can be found in the Supplementary Materials. The transition metal Fe-derived control sample (Fe/N/C) was synthesized according to literatures (*11*, *46*). Specifically, 100 mg of zeolitic imidazolate frameworks (ZIF8), together with 10 mg of tris(1, 10-phenanthroline) iron(II) perchlorate ion, was ball-milled for 1 hour and heated in Ar at 1000°C for 1 hour and then at 900°C under NH_3 for 15 min.

The electrochemical performances of the above ORR catalysts were characterized through (i) half-cell tests in 0.1 M KOH or 0.1 M $HClO_4$ electrolytes by an RDE method and (ii) single-cell tests with a 5-cm^2 MEA and pure H_2/O_2 as fuels at 80°C, 100% relative humidity, and 2-bar back pressure. Detailed electrode fabrication and test processes are described in the Supplementary Materials. The morphology and composition characterization of the materials are also given in the Supplementary Materials.

SUPPLEMENTARY MATERIALS

Supplementary material for this article is available at http://advances.sciencemag.org/cgi/content/full/1/1/e1400129/DC1

Fig. S1. Characterization of VA-NCNTs.

Fig. S2. Electrocatalytic activities of the VA-NCNT catalyst in alkaline electrolyte (O_2-saturated 0.1 M KOH) by half-cell tests.

Fig. S3. Electrocatalytic activities of the VA-NCNT catalyst in acidic electrolyte (O_2-saturated 0.1 M $HClO_4$) by half-cell tests.

Fig. S4. Typical cross-section SEM images of the GDL with the MEA of VA-NCNTs as the cathode catalyst layer, Nafion membrane (N211) as the separator, and Pt/C as the anode.

Fig. S5. SEM (A) and TEM (B) images of N-CNT bundles.

Fig. S6. Typical cross-section SEM images of the GDLs with the MEAs of (A to C) N-G-CNT (2 mg cm^{-2}) and (D to F) N-G-CNT + KB (0.5 + 2 mg cm^{-2}) as the cathode catalyst layers, respectively.

Fig. S7. Tafel plot (A) and electron transfer number (B) for the N-G-CNT and Pt/C (20%) as the function of electrode potential by RRDE in oxygen-saturated 0.1 M KOH solution at a scan speed of 5 mV s^{-1} and a rotation speed of 1600 rpm.

Fig. S8. Long-time stability and tolerance to methanol/carbon monoxide of metal-free catalyst N-G-CNT.

Fig. S9. SEM images of catalyst layer cross sections used in RDE measurements.

Fig. S10. Electrocatalytic activities of the carbon-based metal-free N-G-CNT catalysts in acidic electrolyte (O_2-saturated 0.1 M $HClO_4$) by half-cell tests.

Fig. S11. Optimization of cathode catalyst layer composition.

Fig. S12. Single-cell performance comparison between N-G-CNT and Fe/N/C catalysts at the same catalyst layer composition: catalyst (0.5 mg cm^{-2})/KB (2 mg cm^{-2})/Nafion (2.5 mg cm^{-2}).

Fig. S13. Polarization curves of the N-G-CNT and individual components of N-G or N-CNT.

Fig. S14. Durability of the catalyst layer composed of metal-free N-G-CNT (2 mg cm^{-2}) + KB (2 mg cm^{-2}) in a PEM fuel cell measured at 0.5 V.

Fig. S15. The metal-free character of N-G-CNT catalyst.

REFERENCES AND NOTES

1. K. P. Gong, F. Du, Z. H. Xia, M. Durstock, L. M. Dai, Nitrogen-doped carbon nanotube arrays with high electrocatalytic activity for oxygen reduction. *Science* **323**, 760–764 (2009).
2. J. L. Shui, N. K. Karan, M. Balasubramanian, S. Y. Li, D. J. Liu, Fe/N/C composite in Li–O_2 battery: Studies of catalytic structure and activity toward oxygen evolution reaction. *J. Am. Chem. Soc.* **134**, 16654–16661 (2012).
3. S. Basu, *Recent Trends in Fuel Cell Science and Technology* (Springer, New York, 2007).
4. H. A. Gasteiger, S. S. Kocha, B. Sompalli, F. T. Wagner, Activity benchmarks and requirements for Pt, Pt-alloy, and non-Pt oxygen reduction catalysts for PEMFCs. *Appl. Catal. B Environ.* **56**, 9–35 (2005).
5. F. Jaouen, J. Herranz, M. Lefèvre, J. P. Dodelet, U. I. Kramm, I. Herrmann, P. Bogdanoff, J. Maruyama, T. Nagaoka, A. Garsuch, J. R. Dahn, T. Olson, S. Pylypenko, P. Atanassov, E. A. Ustinov, Cross-laboratory experimental study of non-noble-metal electrocatalysts for the oxygen reduction reaction. *ACS Appl. Mater. Inter.* **1**, 1623–1639 (2009).
6. A. J. Appleby, Electrocatalysis of aqueous dioxygen reduction. *J. Electroanal. Chem.* **357**, 117–179 (1993).
7. R. Adzic, *Recent Advances in the Kinetics of Oxygen Reduction in Electrocatalysis* (Wiley-VCH, New York, 1998).
8. P. Somasundaran, *Encyclopedia of Surface and Colloid Science* (Taylor & Francis, New York, ed. 2, 2006).
9. M. K. Debe, Electrocatalyst approaches and challenges for automotive fuel cells. *Nature* **486**, 43–51 (2012).
10. R. Jasinski, A new fuel cell cathode catalyst. *Nature* **201**, 1212–1213 (1964).
11. E. Proietti, F. Jaouen, M. Lefèvre, N. Larouche, J. Tian, J. Herranz, J. P. Dodelet, Iron-based cathode catalyst with enhanced power density in polymer electrolyte membrane fuel cells. *Nat. Commun.* **2**, 416 (2011).
12. C. Chen, Y. Kang, Z. Huo, Z. Zhu, W. Huang, H. L. Xin, J. D. Snyder, D. Li, J. A. Herron, M. Mavrikakis, M. Chi, K. L. More, Y. Li, N. M. Markovic, G. A. Somorjai, P. Yang, V. R. Stamenkovic, Highly crystalline multimetallic nanoframes with three-dimensional electrocatalytic surfaces. *Science* **343**, 1339–1343 (2014).
13. M. Lefevre, E. Proietti, F. Jaouen, J. P. Dodelet, Iron-based catalysts with improved oxygen reduction activity in polymer electrolyte fuel cells. *Science* **324**, 71–74 (2009).
14. G. Wu, K. L. More, C. M. Johnston, P. Zelenay, High-performance electrocatalysts for oxygen reduction derived from polyaniline, iron, and cobalt. *Science* **332**, 443–447 (2011).
15. S. B. Yang, X. L. Feng, X. C. Wang, K. Mullen, Graphene-based carbon nitride nanosheets as efficient metal-free electrocatalysts for oxygen reduction reactions. *Angew. Chem. Int. Ed.* **50**, 5339–5343 (2011).
16. L. T. Qu, Y. Liu, J. B. Baek, L. M. Dai, Nitrogen-doped graphene as efficient metal-free electrocatalyst for oxygen reduction in fuel cells. *ACS Nano* **4**, 1321–1326 (2010).
17. S. Wang, L. Zhang, Z. Xia, A. Roy, D. W. Chang, J. B. Baek, L. Dai, BCN graphene as efficient metal-free electrocatalyst for the oxygen reduction reaction. *Angew. Chem. Int. Ed.* **51**, 4209–4212 (2012).
18. Y. Zheng, Y. Jiao, M. Jaroniec, Y. G. Jin, S. Z. Qiao, Nanostructured metal-free electrochemical catalysts for highly efficient oxygen reduction. *Small* **8**, 3550–3566 (2012).
19. L. Yang, S. Jiang, Y. Zhao, L. Zhu, S. Chen, X. Wang, Q. Wu, J. Ma, Y. Ma, Z. Hu, Boron-doped carbon nanotubes as metal-free electrocatalysts for the oxygen reduction reaction. *Angew. Chem. Int. Ed.* **50**, 7132–7135 (2011).
20. C. Z. Zhu, S. J. Dong, Recent progress in graphene-based nanomaterials as advanced electrocatalysts towards oxygen reduction reaction. *Nanoscale* **5**, 1753–1767 (2013).
21. X. Q. Wang, J. S. Lee, Q. Zhu, J. Liu, Y. Wang, S. Dai, Ammonia-treated ordered mesoporous carbons as catalytic materials for oxygen reduction reaction. *Chem. Mater.* **22**, 2178–2180 (2010).
22. G. Liu, X. G. Li, J. W. Lee, B. N. Popov, A review of the development of nitrogen-modified carbon-based catalysts for oxygen reduction at USC. *Catal. Sci. Technol.* **1**, 207–217 (2011).
23. R. A. Sidik, A. B. Anderson, N. P. Subramanian, S. P. Kumaraguru, B. N. Popov, O_2 reduction on graphite and nitrogen-doped graphite: Experiment and theory. *J. Phys. Chem. B* **110**, 1787–1793 (2006).
24. Z. W. Liu, F. Peng, H. J. Wang, H. Yu, W. X. Zheng, J. Yang, Phosphorus-doped graphite layers with high electrocatalytic activity for the O_2 reduction in an alkaline medium. *Angew. Chem. Int. Ed.* **50**, 3257–3261 (2011).
25. I. Y. Jeon, H. J. Choi, M. J. Ju, I. T. Choi, K. Lim, J. Ko, H. K. Kim, J. C. Kim, J. J. Lee, D. Shin, S. M. Jung, J. M. Seo, M. J. Kim, N. Park, L. Dai, J. B. Baek, Direct nitrogen fixation at the edges of graphene nanoplatelets as efficient electrocatalysts for energy conversion. *Sci. Rep.* **3**, 2260 (2013).
26. I. Y. Jeon, H. J. Choi, M. Choi, J. M. Seo, S. M. Jung, M. J. Kim, S. Zhang, L. Zhang, Z. Xia, L. Dai, N. Park, J. B. Baek, Facile, scalable synthesis of edge-halogenated graphene nanoplatelets as efficient metal-free eletrocatalysts for oxygen reduction reaction. *Sci. Rep.* **3**, 1810 (2013).
27. I. Y. Jeon, S. Zhang, L. Zhang, H. J. Choi, J. M. Seo, Z. Xia, L. Dai, J. B. Baek, Edge-selectively sulfurized graphene nanoplatelets as efficient metal-free electrocatalysts for oxygen reduction reaction: The electron spin effect. *Adv. Mater.* **25**, 6138–6145 (2013).
28. I. Y. Jeon, H. J. Choi, S. M. Jung, J. M. Seo, M. J. Kim, L. Dai, J. B. Baek, Large-scale production of edge-selectively functionalized graphene nanoplatelets via ball milling and their use as metal-free electrocatalysts for oxygen reduction reaction. *J. Am. Chem. Soc.* **135**, 1386–1393 (2013).
29. Y. Li, J. Wang, X. Li, J. Liu, D. Geng, J. Yang, R. Li, X. Sun, Nitrogen-doped carbon nanotubes as cathode for lithium–air batteries. *Electrochem. Commun.* **13**, 668–672 (2011).

30. J. L. Shui, F. Du, C. M. Xue, Q. Li, L. M. Dai, Vertically aligned N-doped coral-like carbon fiber arrays as efficient air electrodes for high-performance nonaqueous Li-O_2 batteries. *ACS Nano* **8**, 3015–3022 (2014).
31. Y. Xue, J. Liu, H. Chen, R. Wang, D. Li, J. Qu, L. Dai, Nitrogen-doped graphene foams as metal-free counter electrodes in high-performance dye-sensitized solar cells. *Angew. Chem. Int. Ed. Engl.* **51**, 12124–12127 (2012).
32. H. T. Chung, C. M. Johnstona, K. Artyushkovab, M. Ferrandonc, D. J. Myersc, P. Zelenay, Cyanamide-derived non-precious metal catalyst for oxygen reduction. *Electrochem. Commun.* **12**, 1792–1795 (2010).
33. C. H. Choi, M. W. Chung, H. C. Kwon, S. H. Park, S. I. Woo, B, N- and P, N-doped graphene as highly active catalysts for oxygen reduction reactions in acidic media. *J. Mater. Chem. A* **1**, 3694–3699 (2013).
34. Q. Wang, Z. Y. Zhou, Y. J. Lai, Y. You, J. G. Liu, X. L. Wu, E. Terefe, C. Chen, L. Song, M. Rauf, N. Tian, S. G. Sun, Phenylenediamine-based FeNx/C catalyst with high activity for oxygen reduction in acid medium and its active-site probing. *J. Am. Chem. Soc.* **136**, 10882–10885 (2014).
35. Y. Jiao, Y. Zheng, M. Jaroniec, S. Z. Qiao, Origin of the Electrocatalytic oxygen reduction activity of graphene-based catalysts: A roadmap to achieve the best performance. *J. Am. Chem. Soc.* **136**, 4394–4403 (2014).
36. L. Li, Y. C. Xing, Electrochemical durability of carbon nanotubes in noncatalyzed and catalyzed oxidations. *J. Electrochem. Soc.* **153**, A1823–A1828 (2006).
37. L. M. Dai, Functionalization of graphene for efficient energy conversion and storage. *Acc. Chem. Res.* **46**, 31–42 (2013), and references cited therein.
38. Z. Yang, Z. Yao, G. Li, G. Fang, H. Nie, Z. Liu, X. Zhou, X. Chen, S. Huang, Sulfur-doped graphene as an efficient metal-free cathode catalyst for oxygen reduction. *ACS Nano* **6**, 205–211 (2012).
39. T. Y. Ma, S. Dai, M. Jaroniec, S. Z. Qiao, Graphitic carbon nitride nanosheet–carbon nanotube three-dimensional porous composites as high-performance oxygen evolution electrocatalysts. *Angew. Chem. Int. Ed.* **53**, 7281–7285 (2014).
40. F. Du, D. Yu, L. Dai, S. Ganguli, V. Varshney, A. K. Roy, Preparation of tunable 3D pillared carbon nanotube-graphene networks for high-performance capacitance. *Chem. Mater.* **23**, 4810–4816 (2011).
41. D. S. Yu, L. M. Dai, Self-assembled graphene/carbon nanotube hybrid films for supercapacitors. *J. Phys. Chem. Lett.* **1**, 467–470 (2010).
42. D. Yu, K. Goh, H. Wang, L. Wei, W. Jiang, Q. Zhang, L. Dai, Y. Chen, Scalable synthesis of hierarchically-structured carbon nanotube-graphene fibres for capacitive energy storage. *Nat. Nanotechnol.* **9**, 555–562 (2014).
43. Y. Xue, D. Yu, L. Dai, R. Wang, D. Li, A. Roy, F. Lu, H. Chen, Y. Liu, J. Qu, Three-dimensional B, N-doped graphene foam as metal-free catalysts for oxygen reduction reaction. *Phys. Chem. Chem. Phys.* **15**, 12220–12226 (2013).
44. G. Wu, C. S. Dai, D. L. Wang, D. Y. Li, N. Li, Nitrogen-doped magnetic onion-like carbon as support for Pt particles in a hybrid cathode catalyst for fuel cells. *J. Mater. Chem.* **20**, 3059–3068 (2010).
45. G. Wu, K. L. More, P. Xu, H. L. Wang, M. Ferrandon, A. J. Kropf, D. J. Myers, S. Ma, C. M. Johnston, P. Zelenay, A carbon-nanotube-supported graphene-rich non-precious metal oxygen reduction catalyst with enhanced performance durability. *Chem. Commun.* **49**, 3291–3293 (2013).
46. D. Zhao, J. L. Shui, L. R. Grabstanowicz, C. Chen, S. M. Commet, T. Xu, J. Lu, D. J. Liu, Highly efficient non-precious metal electrocatalysts prepared from one-pot synthesized zeolitic imidazolate frameworks. *Adv. Mater.* **26**, 1093–1097 (2014).

Acknowledgments: We thank the support from the National Science Foundation (Accelerating Innovation Research-IIP-1343270 and CMMI-1266295).

Submitted 20 November 2014
Accepted 24 January 2015
Published 27 February 2015
10.1126/sciadv.1400129

Citation: Shui *et al*., N-doped carbon nanomaterials are durable catalysts for oxygen reduction reaction in acidic fuel cells. *Sci. Adv.* **1**, e1400129 (2015).